ELSEVIER

www.elsevier.nl/locate/carres

Carbohydrate Research 329 (2000) 131–139

CARBOHYDRATE RESEARCH

Boat conformations. Analysis and simulation of the complex ^{1}H NMR spectrum of methyl 2,6:3,4-dianhydro-α-D-altropyranoside☆

Bruce Coxon *

Biotechnology Division, National Institute of Standards and Technology, 100 Bureau Drive Stop 8311, Gaithersburg, MD 20899-8311, USA

Received 7 March 2000; accepted 25 May 2000

Abstract

The complex ^{1}H NMR spectrum of methyl 2,6:3,4-dianhydro-α-D-altropyranoside (**1**) has been analyzed and simulated in detail by using input parameters derived from experimental ^{1}H chemical shifts, long- and short-range coupling constants, spin–lattice relaxation times, and effective, spin–spin relaxation times obtained by trial and error matching of the experimental and simulated spectra. The ^{13}C spin–lattice relaxation times of **1** have also been measured, and along with the ^{1}H–^{1}H long- and short-range coupling constants, have been interpreted in terms of the geometry of **1** defined by molecular dynamics with simulated annealing.

Keywords: Altropyranoside; Boat conformations; Carbon-13–proton chemical shift correlation; 2,6:3,4-Dianhydride; Gradient-enhanced 2D HSQC; Long-range coupling constants; Molecular dynamics; Simulated annealing; Spin–lattice relaxation times

1. Introduction

Bridged ring structures of carbohydrates are unique templates for studies of the dependence of homo- and heteronuclear coupling constants on atomic dihedral angle, particularly if such structures exhibit a degree of rigidity that prevents contributions to the coupling constants from equilibria with alternative conformational populations. In previous work, we studied the geometry of the skew boat conformation of 3-*O*-benzoyl-1,2,4-*O*-benzylidyne-α-D-ribopyranose [1], and also that of a more classical boat conformation of methyl 2,6-anhydro-3-deoxy-3-phthalimido-α-D-mannopyranoside [2]. The latter derivative was synthesized from methyl 2,6:3,4-dianhydro-α-D-altropyranoside (**1**) in ^{15}N-labeled form, for the purpose of studying the angular dependence of vicinal ^{15}N–^{1}H coupling constants in carbohydrates. During the course of these studies, we noticed that the resolution-enhanced ^{1}H NMR spectrum of dianhydride **1** is unusually complex for a simple carbohydrate derivative, and it seemed worthwhile to make a detailed analysis and simulation of this spectrum, with the objective of revealing a number of stereochemically well defined NMR coupling constants that could be useful in the industrial analysis of carbohydrates and aminoglycoside antibiotics.

☆ Part III of a series: Boat conformations. For Parts I and II, see Refs. [1] and [2].

* Tel.: +1-301-9753135; fax: +1-301-3303447.
E-mail address: bruce.coxon@nist.gov (B. Coxon).

0008-6215/00/$ - see front matter
PII: S0008-6215(00)00173-7

Table 1
^{1}H and ^{13}C NMR chemical shifts [a] and spin–lattice relaxation times, and ^{1}H spin–spin relaxation times of methyl 2,6:3,4-dianhydro-α-D-altropyranoside (**1**)

Position							
1	2	3	4	5	6	6′	OMe
^{1}H chemical shift [b]							
4.9501 ± 0.0001	4.1184 ± 0.0002	3.6255 ± 0.0004	3.4278 ± 0.0004	4.3761 ± 0.0003	3.9994 ± 0.0001	3.6655 ± 0.0002	3.4995 ± 0.0001
^{13}C chemical shift [c]							
103.163 ± 0.002	68.677 ± 0.002	48.104 ± 0.002	48.952 ± 0.002	66.158 ± 0.002	63.297 ± 0.002		56.883 ± 0.002
Non-selective ^{1}H spin–lattice relaxation time [d] (T_1, s)							
4.19 ± 0.04	4.89 ± 0.06	5.01 ± 0.05	4.75 ± 0.06	4.36 ± 0.04	2.33 ± 0.02	2.31 ± 0.03	3.10 ± 0.03
^{13}C spin–lattice relaxation time [e] (T_1, s)							
Measured							
4.79 ± 0.13	4.56 ± 0.05	4.28 ± 0.05	3.89 ± 0.02	4.50 ± 0.05	2.22 ± 0.02		5.94 ± 0.14
Calculated							
4.62	4.56	4.31	4.29	4.50	2.34		
Effective ^{1}H spin–spin relaxation time [f] (T_2^*, s)							
0.44	0.30	0.43	0.41	0.35	0.42	0.33	[g]

[a] In ppm from internal Me_4Si at 300 K.
[b] Mean of five measurements at 600 MHz, ± standard uncertainty.
[c] Mean of six measurements at 151 MHz/600 MHz, ± standard uncertainty.
[d] Mean of 12 measurements at 600 MHz, ± standard uncertainty.
[e] Mean of eight measurements at 151 MHz/600 MHz, ± standard uncertainty.
[f] Determined by matching of line-widths and line-shapes in the spectrum simulation.
[g] Not simulated.

Table 2
^{1}H–^{1}H NMR coupling constants [a] (Hz, without relative signs) of methyl 2,6:3,4-dianhydro-α-D-altropyranoside (**1**)

Vicinal and geminal							Long-range (>3 bonds)						
$J_{1,2}$	$J_{2,3}$	$J_{3,4}$	$J_{4,5}$	$J_{5,6}$	$J_{5,6'}$	$J_{6,6'}$	$J_{1,3}$	$J_{1,4}$	$J_{2,4}$	$J_{2,5}$	$J_{2,6}$	$J_{3,5}$	$J_{4,6}$
2.3	4.05	4.7	3.0	2.35	1.0	9.6	1.6	0.5	0.5	0.25	0.5	0.6	0.5

[a] Measured at 600 MHz with an estimated standard uncertainty of 0.1 Hz, except for $J_{2,5}$, which was measured at 400 MHz.

Compound **1** was first synthesized by Sinclair [3], but only a limited NMR study was done. As part of our study, we have determined the ^{1}H chemical shifts, coupling constants, non-selective longitudinal and effective transverse relaxation times, and ^{13}C chemical shifts and longitudinal relaxation times for **1**. The experimental ^{1}H NMR parameters have been used as input for simulation of the ^{1}H spectrum of **1** as a seven-spin system, and have been interpreted in terms of a geometry of **1** obtained by molecular dynamics with simulated annealing.

2. Results and discussion

NMR spectroscopy.—Under drastic resolution enhancement using a line-broadening of −3 Hz, the well dispersed H-1, H-2, H-3, H-4, H-5, H-6[1], and H-6′ NMR signals of **1** at 400 MHz or 600 MHz appeared as 7, 16, 14, 15, 10, 12, and 4 line multiplets, respectively. This complexity indicates the presence of measurable long-range, ^{1}H–^{1}H coupling (over

[1] H-6 is defined as the signal at lower field, and H-6′ as that at higher field.

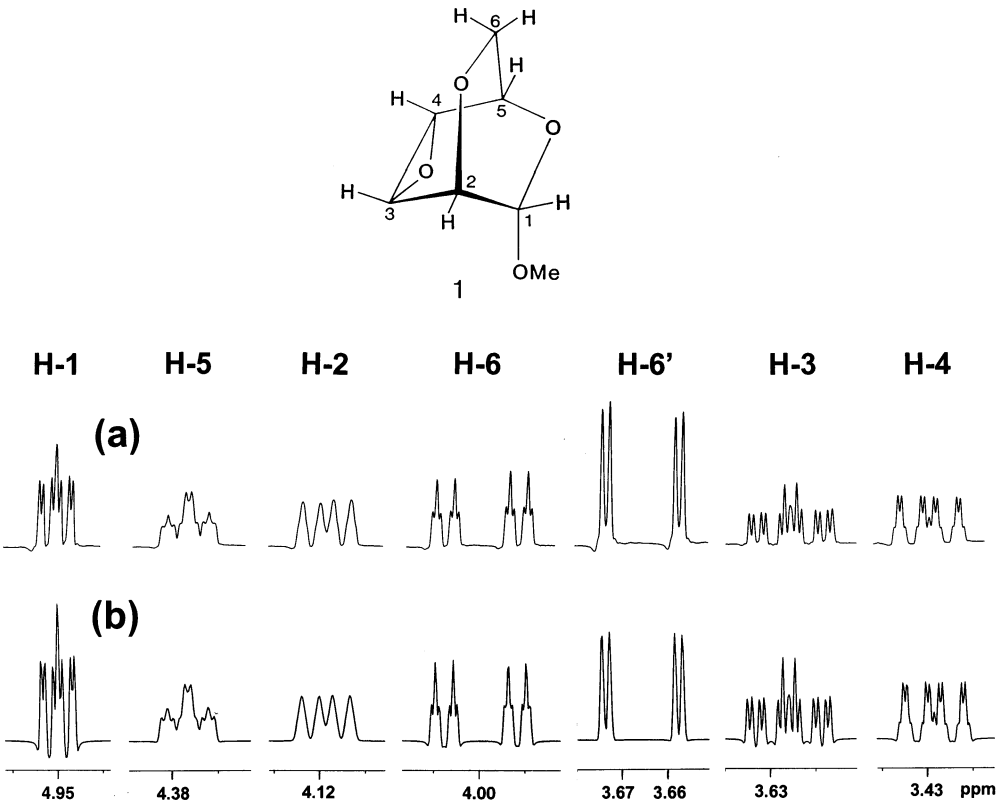

Fig. 1. ^{1}H NMR spectra of methyl 2,6:3,4-dianhydro-α-D-altropyranoside (**1**) at 600 MHz, with moderate resolution enhancement applied by Gaussian filtering with a line-broadening of −1.0 Hz; (a) experimental spectrum, (b) simulated spectrum. The methoxyl resonance is not shown.

more than three bonds) for all protons except H-6′. Matching of multiplet spacings and homonuclear spin decoupling experiments led to the ^{1}H chemical shift assignments shown in Table 1, and the ^{1}H–^{1}H coupling constant values reported in Table 2. Non-selective ^{1}H and ^{13}C spin–lattice relaxation times were measured for **1**, and are shown in Table 1. ^{13}C chemical shift assignments for **1** were made by the sensitivity-enhanced, *z*-gradient two-dimensional (2D) heteronuclear single quantum correlation (HSQC) method [4,5], and are reported in Table 1.

Spectral simulation.—The 600 MHz spectrum of the ring protons of **1** obtained by processing the experimental NMR data with moderate resolution enhancement (line-broadening of −1 Hz) is shown in Fig. 1(a). The more drastic resolution enhancement mentioned before is not shown here because of the resultant severe baseline distortion in and around the multiplets. Simulation of the ^{1}H NMR spectrum of **1** was achieved by means of a modern NMR program that calculates a free induction decay signal from an input of ^{1}H chemical shifts, coupling constants, and spin–lattice (T_1) and effective spin–spin (T_2^*) relaxation times. Input for the first three parameters was obtained from the experimental data, whereas the T_2^* values (shown in Table 1) were determined separately for each multiplet by trial and error adjustment, until the multiplet shapes and line widths in the simulated spectrum matched those in the experimental spectrum. A very good match of experimental (Fig. 1(a)) and simulated (Fig. 1(b)) spectra was obtained, which suggests that the analysis of the complex ^{1}H NMR spectrum of **1** is correct.

Molecular modeling.—Application of a molecular dynamics computation to **1** with simulated annealing and energy minimization according to a modified AMBER forcefield with Homans' carbohydrate parameters [6] and epoxide atom types, indicated two rotameric states of the methoxyl group (see Fig. 2). In one of these, the methoxyl carbon atom is approximately trans to C-2 (see Fig. 2(a,b)),

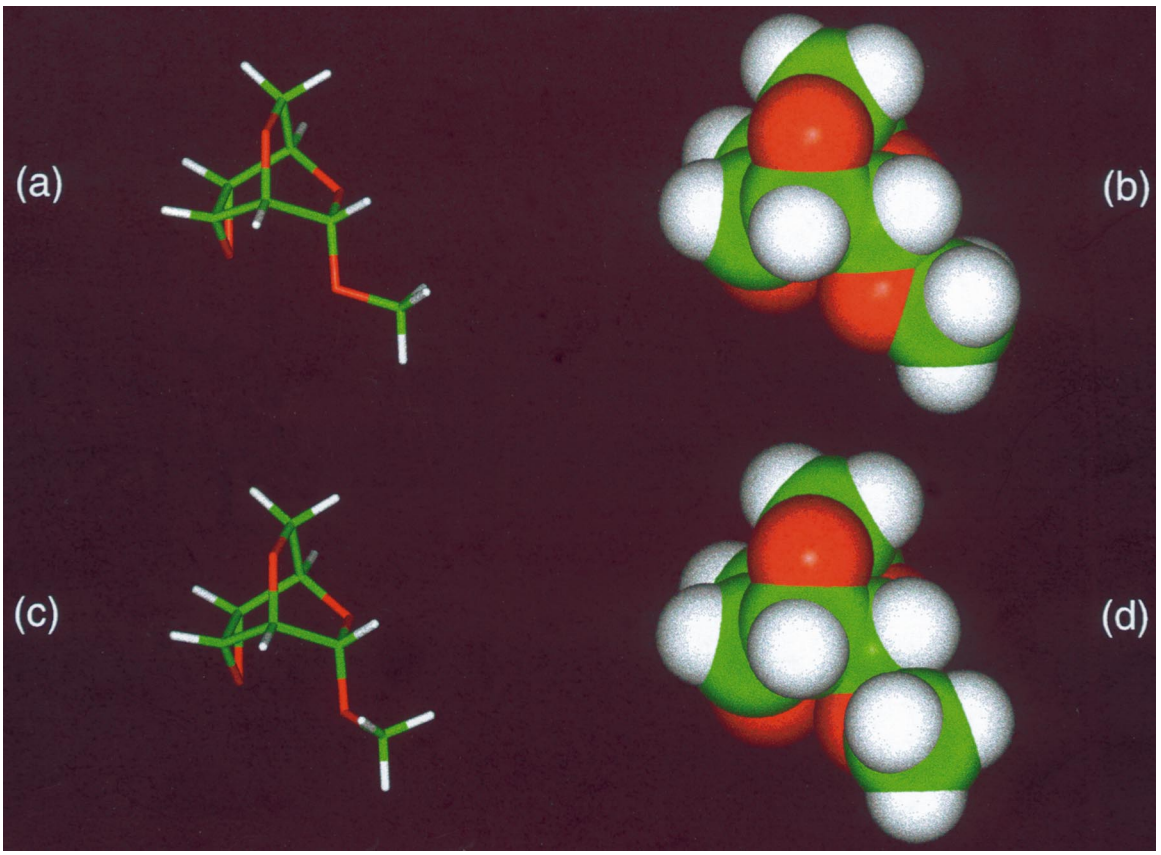

Fig. 2. Two methoxyl rotamers of methyl 2,6:3,4-dianhydro-α-D-altropyranoside (**1**) obtained by molecular dynamics with simulated annealing, and energy minimization by means of a modified AMBER forcefield with epoxide atom types and Homans' carbohydrate parameters; (a) and (b), stick and space-filling models of the more stable rotamer in which the methyl carbon atom is ca. trans to C-2; (c) and (d), stick and space-filling models of the less stable rotamer in which the methyl carbon atom is ca. trans to O-5.

Table 3
Dihedral angles [a] (°) of methoxyl rotamers of methyl 2,6:3,4-dianhydro-α-D-altropyranoside (**1**) obtained from molecular dynamics models [b]

Atom pair	H-1,H-2	H-2,H-3	H-3,H-4	H-4,H-5	H-5,H-6	H-5,H-6′	C-2,O*C*H$_3$
C-2,O*C*H$_3$ trans rotamer	−66.4	53.2	0.3	−54.2	−61.4	60.1	−161.6
O-5,O*C*H$_3$ trans rotamer	−66.9	53.2	0.3	−54.2	−61.5	60.1	−105.5

[a] Estimated standard uncertainty 0.1°.
[b] Energy minimization with a modified AMBER forcefield with epoxide atom types included and Homans' parameters for the anomeric atoms.

with a dihedral angle ϕ(C-2,O*C*H$_3$) −161.6°. This rotamer is only slightly more stable by 0.84 kJ/mol (0.20 kcal/mol) than another (see Fig. 2(c,d)) in which the methoxyl carbon atom is approximately trans to O-5, and in which ϕ(C-2,O*C*H$_3$) is −105.5° [ϕ(O-5,O*C*H$_3$) = 133.4°]. From the relationship $\Delta G = -RT \ln K$, a free energy difference of 0.84 kJ/mol corresponds to a rotamer ratio of 29:21 in favor of the C-2,O*C*H$_3$ trans rotamer (see Fig. 2(a,b)). The ^{1}H–^{1}H dihedral angles for these methoxyl rotamers are shown in Table 3.

Apparently, it is the inclusion of the Homans' forcefield parameters for the anomeric atoms that directs the modeling computation towards favoring the C-2,O*C*H$_3$ trans rotamer, because an alternative computation using a consistent forcefield that included epoxide atom types, but no Homans'

parameters yielded a pair of rotamers where the O-5,OCH_3 trans form was more stable than the C-2,OCH_3 trans form by 0.58 kJ/mol (0.14 kcal/mol). However, the computation with the AMBER/Homans forcefield is believed to be the better treatment, because it allows for the anomeric effect in carbohydrates.

Evidently, the fusion of an essentially planar epoxide ring to the pyranoid boat form of **1** introduces additional rigidity into the bicyclic system. According to the molecular dynamics models, the 'gunwale' dihedral angle $\phi_{3,4}$ is only 0.3° in **1**, but in the models of a series of non-epoxide methyl 2,6-anhydro-α-D-altropyranoside derivatives and methyl 2,6-anhydro-3-deoxy-3-phthalimido-α-D-mannopyranoside [2], we have found that this angle is typically in the range 10–16° [7]. This effect appears to be due to distortion of the classical, pyranoid boat conformation of the non-epoxide 2,6-anhydrohexopyranoside derivatives towards a skew form, presumably to relieve eclipsed, non-bonded interactions. Thus in one sense, the epoxide **1** is a better template for studies of the angular dependence of coupling constants, because its molecular framework is more rigid than that of many 2,6-anhydrohexopyranosides.

^1H and ^{13}C chemical shifts.—As pointed out by Sinclair [3], the epoxide protons H-3 and H-4 of **1** resonate at higher field than do the other ring protons (see Fig. 1 and Table 1). This may be attributed to the presence of a small ring current in the epoxide ring [8] which shields H-3 and H-4 at their location defined by a dihedral angle of 67–68° above the plane of this ring (see Fig. 2). A similar, but larger effect was observed for the ^{13}C chemical shifts of C-3 and C-4, which resonate 17–21 ppm to higher field than C-2 and C-5 (see Table 1). Although in the forcefield used in the molecular modeling, the epoxide ring bonds were formally treated as being sp^3 hybridized, by analogy with cyclopropane [9], they may well be closer to sp^5, with increased p character that facilitates electron delocalization in the epoxide ring.

^1H and ^{13}C spin–lattice relaxation times.—The ^1H and ^{13}C T_1 values for **1** (see Table 1) are quite long, but are generally of the same order, except for the $^{13}CH_3$ T_1, which is almost twice as long as the methyl proton T_1, presumably because of inefficient relaxation of the methyl carbon nucleus by the dipolar and spin rotation mechanisms. Very similar T_1 values were observed for the methylene protons and methylene carbon nucleus, owing to the similar effects of short-range, dipolar relaxation. The approximately two-fold increase in relaxation rate for these nuclei compared with the other ring nuclei is undoubtedly due on the one hand to strong relaxation of H-6 and H-6′ by each other over a short inter-proton distance of 1.8 Å (molecular dynamics model), and on the other, to efficient relaxation of C-6 by its two directly bonded protons. The similarity of the methine ^{13}C T_1 values for **1** (see Table 1) indicates that this molecule tumbles isotropically [10].

A rotational correlation time (τ_c) for a typical ring carbon nucleus (C-2) in the fast motion limit was calculated from the relaxation rate equation

$$1/T_1 = \Sigma_{i=1 \text{ to } n} \gamma_H^2 \gamma_C^2 \hbar^2 (\mu_0/4\pi)^2 \tau_c / r_{C,H(i)}^6$$

where [11] $\gamma_H = 2.6751987 \times 10^8$ rad/T per s, $\gamma_C = 6.72822 \times 10^7$ rad/T per s, $\hbar = 1.0546 \times 10^{-34}$ J s, and the vacuum permeability $\mu_0 = 4\pi \times 10^{-7}$ T m/A, and where the carbon–proton distances $r_{C,H(i)}$ measured from the molecular dynamics model (see Fig. 2(a,b)) were summed over all of the ring protons ($i = 1,2,...6'$) that were believed to contribute to the relaxation of ^{13}C-2. Because the methyl ^{13}C T_1 5.94 s is significantly longer than the ring carbon T_1s (see Table 1), it was assumed that neither the dipolar nor spin rotation relaxation mechanisms are particularly effective for the methyl ^{13}C, and, therefore, are likely to be even less effective for relaxation of the more remote ring ^{13}C nuclei, including ^{13}C-2. Therefore, no term for relaxation by the methyl protons was included in the summation. This calculation yielded a rotational correlation time τ_c 10.4 ps, which is short as anticipated, because compound **1** is a small, almost globular molecule that is expected to reorient rapidly. The longer correlation times τ_c 18.2 and 26.0 ps, respectively, for 3,4,6-tri-*O*-acetyl-1,2-*O*-(1-methoxyethylidene)-β-D-mannopyranose and 3,4,6-tri-*O*-

acetyl - 1,2 - *O* - (1 - benzyloxyethylidene) - β - D-mannopyranose may be compared [10].

By using the correlation time for ^{13}C-2, the relaxation rate equation was then used to back-calculate ^{13}C T_1 values for the remaining ring ^{13}C nuclei by summing the relaxation contributions from ring protons at various distances in the model for each ring ^{13}C. Again, the methyl protons were excluded from these calculations. The back-calculated ^{13}C T_1 values may be compared with the experimental values in Table 1. Good-to-fair agreement was obtained for the most part, but the experimental T_1 3.89 s for C-4 is significantly shorter than the calculated value of 4.29 s. The closer proximity of the H-6 and H-6′ protons to C-4 than to C-3 does not make much difference to the calculated C-4 T_1 value. However, because of the $r^6_{C,H(i)}$ dependence in the relaxation rate equation, ^{13}C T_1 values are known to be very sensitive to C–H bond length [12]. The fact that the experimental T_1 4.79 s for ^{13}C-1 is longer than the calculated value of 4.62 s supports the notion that the methyl proton relaxation contribution is negligible.

The effective, ^{1}H spin–spin relaxation times T_2^* determined by simulation (see Table 1) are quite similar, and do not appear to be particularly diagnostic for proton type or location.

^{1}H–^{1}H coupling constants.—The configuration of **1** is unique in that all of the hydrogen atoms on the pyranoid ring are equatorial, leading to extensive, long-range coupling. The magnitudes of the vicinal, methine proton–methine proton coupling constants (see Table 2) reflect expectations based on a Karplus dependence [13–15] on the dihedral angles (see Table 3) obtained from the molecular dynamics model. Thus $J_{1,2}$ is smaller than $J_{2,3}$ and $J_{4,5}$ partly because the modeling indicates that $|\phi_{1,2}$ 66.4°$|$ is larger than $\phi_{2,3}$ 53.2° and $|\phi_{4,5}$ 54.2°$|$, and partly because of the additional electronegativity of O-1. For an almost zero dihedral angle of $\phi_{3,4}$ 0.3°, the value $J_{3,4}$ 4.7 Hz is characteristically small, as are the cis vicinal couplings of other epoxides [8]. Attenuation of these couplings by the electronegativity of the epoxide oxygen atom has required interpretation by means of a revised Karplus equation [8].

From the data in Table 2, it may be seen that $J_{5,6}$ 2.35 Hz and $J_{5,6'}$ 1.0 Hz are markedly different, despite the modeling result (Table 3) that $|\phi_{5,6}$ 61.4°$|$ and $\phi_{5,6'}$ 60.1° are very similar. We have found that this difference is characteristic in a series of methyl 2,6-anhydro-α-D-altropyranosides [7], and in methyl 2,6-anhydro-3-deoxy-3-phthalimido-α-D-mannopyranoside [2], and cannot be attributed to differing dihedral angles of H-5,H-6, and H-5,H-6′.

The largest long-range coupling constant observed for **1** (see Table 2) is $J_{1,3}$ 1.6 Hz, which is a typical example of a four-bond coupling of the planar 'W' type, with a magnitude perhaps enhanced in **1** and in a series of methyl 2,6-anhydro-α-D-altropyranosides [7], by the rigidity of the structures. Because such coupling constants clearly have a strong dependence on dihedral angle, the indirect, through-bond mechanism is thought to be more important than the direct, through-space mechanism. From the molecular dynamics models of **1** (see Fig. 2), the relevant dihedral angles were measured as ϕ' 170.8° and ϕ''' 175.6° for the C-2,OCH_3 trans rotamer, and ϕ' 170.2° and ϕ''' 175.6° for the O-5,OCH_3 trans rotamer, where ϕ' is the dihedral angle of H-1 and C-3 about the C-1–C-2 bond, and ϕ''' is the dihedral angle of H-3 and C-1 about the C-2–C-3 bond. Application of Barfield's equation

$$^4J = 0.7(\cos^2\phi' + \cos^2\phi''') - 0.3$$

for the indirect contribution to the coupling [16,17] yielded a theoretical value $J_{1,3}$ 1.1 Hz for both rotamers of **1**, which underestimates the experimental value. On the other hand, overestimated values of $J_{1,3}$ 3.1 Hz were obtained for the rotamers by calculation of the Bystrov and Stepanyants equation

$$^4J = 3.61\cos^2\phi'\cos^2\phi''' - 0.35$$

where $90° \leq \phi', \phi''' \leq 180°$, despite that fact that this empirical equation [17] was designed from data for bicyclo[2,2,1]heptene derivatives, having structures that are not unlike that of **1**.

Owing to the presumed electron delocalization in the epoxide ring and the likely enhanced p character of its ring bonds, the

structure of **1** might be considered to resemble that of a 3-enohexopyranoside. From this viewpoint, the four-bond, long-range couplings $J_{2,4}$ 0.5 Hz and $J_{3,5}$ 0.6 Hz of **1** (Table 2) could be considered to be analogous to allylic couplings across double bonds, and the five-bond coupling $J_{2,5}$ 0.25 Hz could be thought of as a biallylic coupling. Previously, we reported a study of allylic and biallylic couplings and their relative signs in methyl 3,4-dichloro-4-deoxy-α-D-*glycero*-pent-2-enopyranoside [18]. We found that the vicinal $J_{1,2}$ 3.1 Hz and biallylic $J_{1,4}$ 1.3 Hz couplings have the same sign, whereas $J_{1,2}$ and the allylic $J_{2,4}$ 1.2 Hz coupling have opposite signs. Simulations of the ^{1}H spectrum of **1** according to the latter criterion were tried, but the results were not perceptibly dependent on whether the coupling constants were set with the same or alternating signs, perhaps owing to the lack of strong coupling in this system at the high Larmor frequencies used. The $J_{2,4}$ 0.5 Hz coupling found in **1** has been observed to be 0.5–0.9 Hz in all other methyl 2,6-anhydro-α-D-altropyranoside derivatives studied, but the $J_{1,4}$ 0.5 Hz coupling in **1** has been observed (0.4 Hz) only in the parent methyl 2,6-anhydro-α-D-altropyranoside [7]. A number of long-range coupling constants were observed for **1** (see Table 2) that have not been observed for other methyl 2,6-anhydro-α-D-altropyranosides [7]. These are $J_{2,5}$ 0.25 Hz, $J_{2,6}$ 0.5 Hz, $J_{3,5}$ 0.6 Hz, and $J_{4,6}$ 0.5 Hz. Although the transmission of these coupling constants is probably enhanced by electron delocalization in the coupling pathway, the magnitudes of the couplings may also be attenuated by the epoxide oxygen atom, since the 'allylic' and 'biallylic' couplings of **1** are smaller than those observed for methyl 3,4-dichloro-4-deoxy-α-D-*glycero*-pent-2-enopyranoside [18].

It is noteworthy that H-2 is coupled to all other ring protons except H-6′, the only proton signal that appears as a simple, sharp quartet (see Fig. 1) with no evidence of any long-range coupling. Apparently, the possibility of efficient, alternative coupling pathways in structures such as **1** may be ruled out. For example, if transmission of coupling information from H-2 to H-6 proceeded through O-6, then coupling of H-2 with H-6′ would also be expected, because H-6 and H-6′ have essentially the same dihedral angle with respect to the coupling pathway H-2–C-2–O-6–C-6. The other possible coupling pathway H-2–C-2–C-1–O-5–C-5–C-6–H-6 also seems unlikely, as it involves six saturated bonds, and the non-observation of any $J_{1,5}$ coupling for **1** suggests that transmission of coupling through O-5 may be attenuated by its electronegativity.

Stereospecific assignment of H-6 and H-6′.—For **1**, the observation of a coupling of H-2 with H-6 but not with H-6′ provides a basis for the stereospecific assignment of the H-6 and H-6′ NMR signals. It is known that planarity of saturated bonds in a spin coupling pathway enhances the transmission of long-range coupling constants over these bonds [16]. Therefore, because transmission of H-2–H-6 coupling is expected to be via the bonds H-2–C-2–C-3–C-4–C-5–C-6–H-6, and not through the aforementioned, alternative coupling pathways through the electronegative O-5 and O-6 atoms, we propose that it is the H-6 proton [(S)-H-6] that lies in the same plane as C-6, C-5, and C-4 that is coupled to H-2, and not the (R)-H-6 proton that lies outside this plane. On this basis, (S)-H-6 is assigned as the lower field quartet of triplets labeled as H-6 in the ^{1}H NMR spectrum (Fig. 1(a)) and (R)-H-6 as the sharp quartet at higher field, labeled as H-6′. Support for this assignment comes from two sources. Firstly, for compound **1** and its related series of methyl 2,6-anhydro-α-D-altropyranoside derivatives [7], the H-6′ proton having the smaller 5,6-coupling constant ($J_{5,6'}$ 0.5–1.0 Hz) always resonates at higher field than the H-6 proton having the larger 5,6-coupling ($J_{5,6}$ 2.3–3.4 Hz). However, in methyl 2,6-anhydro-3-deoxy-3-phthalimido-α-D-mannopyranoside, these chemical shift positions are reversed, a change that may be attributed to the proximity of (R)-H-6 to a deshielding, carbonyl plane in the particular phthalimido rotamer of the α-D-mannopyranoside derivative that was indicated by modeling [2]. Secondly, the fact that it is (R)-H-6 that displays the smaller 5,6-coupling constant is consistent with its trans coplanar orientation to O-5. In this position, (R)-H-6 would be expected to experience Booth's electronegativity orientation effect

[15,19], which is known to diminish the magnitudes of the vicinal coupling constants of proton pairs in which one of the protons is trans coplanar to an electronegative atom. This analysis also indicates that the previously unassigned H-6 signals of methyl 2,6-anhydro-3-deoxy-3-phthalimido-α-D-mannopyranoside [2] at lower field (δ 4.398) and higher field (δ 4.048) may be stereospecifically assigned as (R)-H-6 and (S)-H-6, respectively.

In summary, the complex ^{1}H NMR spectrum of **1** has been analyzed and simulated in detail by using input parameters derived from experimental ^{1}H chemical shifts, long- and short-range coupling constants, spin–lattice relaxation times, and empirically determined, effective spin–spin relaxation times. The ^{13}C spin–lattice relaxation times of **1** have also been measured, and along with the ^{1}H–^{1}H long- and short-range coupling constants, have been interpreted in terms of a geometry of **1** determined by molecular dynamics with simulated annealing. Analysis of the long- and short-range coupling constants has also indicated a stereospecific assignment of the H-6 and H-6′ ^{1}H NMR signals of **1**. The NMR parameters obtained from the essentially rigid, tricyclic ring system of **1** should be useful in the NMR analysis of biologically important carbohydrates.

3. Experimental

Materials.—Compound **1** was prepared as described by Sinclair [3], except that sublimation under reduced pressure at 70–80 °C was found to be a valuable purification method for **1**; mp 80.7–81.4 °C, lit [3] mp 78–80 °C.

NMR spectroscopy.—One-dimensional ^{1}H and ^{13}C NMR spectra were recorded at 300 K by use of Bruker Instruments[2] WM-400 and DRX-600 NMR spectrometers, as described previously [2]. A solution of **1** (10 mg) in chloroform-*d* (0.4 mL) was used that contained 1% v/v Me_4Si as an internal reference. ^{1}H chemical shift and coupling constant assignments were confirmed by homonuclear, spin-decoupling experiments at 400 MHz. ^{13}C NMR assignments were obtained by ^{13}C/^{1}H chemical shift correlation, using sensitivity-enhanced, *z*-gradient 2D HSQC [4,5] at 150.9/600.13 MHz, as described previously [2].

Measurement of NMR relaxation times.—^{1}H spin–lattice relaxation times (T_1) were measured by the inversion recovery (IR) method [20] at 600.13 MHz. A spectral width of 5.21 kHz was used with a data size of 16,384 points, a 90° pulse width of 10.9 μs, four dummy scans and eight observation scans per spectrum, a data acquisition time of 1.57 s, and a relaxation delay of 15 s. The variable delay schedule was 0.0001, 15, 0.001, 10, 0.002, 5, 0.005, 2, 0.01, 1, 0.02, 0.75, 0.05, 0.5, 0.1, 1.25, 0.4, 3, 0.2, and 1.5 s.

^{13}C T_1 values were measured for **1** (51 mg) in chloroform-*d* (0.4 mL) solution by using the IR method at 150.9 MHz, with WALTZ-16 composite pulse ^{1}H decoupling [21] at 600 MHz, and an inverse, triple resonance probe with ^{13}C observation via the ^{13}C decoupling coil. A spectral width of 18.1 kHz was used with a 32,768 point data set, a 90° pulse width of 16.5 μs, a data acquisition time of 0.9 s, 24 scans/spectrum, and a relaxation delay of 15 s. The variable delay sequence was 0.0001, 15, 0.001, 10, 0.1, 3, 0.5, 5, 1, 4.5, 1.5, 4, 2, 3.5, 2.5, and 7.5 s. All spin–lattice relaxation data were acquired and processed in the 2D mode of the Bruker XWINNMR program version 2.5, and were then analyzed in the T_1/T_2 module of this program, by use of a three-parameter fit.

Spectral simulation.—The ^{1}H NMR spectrum of **1** at 600 MHz was simulated as a seven-spin system, i.e., without the methyl group, by means of the Bruker NMRSIM program version 2.7, running on a SGI Indigo 2 R-4400 workstation equipped with a 250 MHz CPU. Experimental ^{1}H chemical shifts, coupling constants, and T_1 values, and also estimated, effective ^{1}H T_2 values (T_2^*) were used as computational input. For comparison of the experimental and simulated ^{1}H NMR spectra of **1** (see Fig. 1), the experimental and theoretical free-induction decays were pro-

[2] Certain commercial equipment, instruments, or materials are identified in this paper to specify adequately the experimental procedure. Such identification does not imply recommendation by the National Institute of Standards and Technology, nor does it imply that the materials are necessarily the best available for the purpose.

cessed in the same way by Gaussian resolution enhancement, using a line broadening of −1.0 Hz, and a Gaussian truncation fraction of 0.3.

Molecular modeling.—Molecular modeling computations were performed with an SGI Indigo 2 R-4400 workstation equipped with a 200 MHz CPU and Molecular Simulations Inc. (MSI)/BIOSYM INSIGHT II/DISCOVER software, versions 950 and 970. Some computations were done with version 980 of this software, running on a SGI multiprocessor system equipped with 11 R-10000 196 MHz CPUs. Three-dimensional structures were built in the MSI/BIOSYM SKETCHER program, version 950, running on an SGI workstation. Energy computations were performed by using the CFF91 forcefield, the AMBER forcefield with Homans' modifications [6] for carbohydrates, or an Amber/Homans' forcefield modified by the inclusion of epoxide carbon atom and oxygen atom types taken from the CFF91 forcefield. The calculations were done with implicit solvent, by using a distance dependent, effective dielectric constant of 4.0. Initially, a steepest descent energy minimization was conducted for 1000 steps, followed by a VA09A minimization, until an r.m.s derivative of < 0.001 was reached. Molecular dynamics with simulated annealing was then performed over the temperature range 1000–300 K, with 50 K decrements. At each temperature, 1000 equilibration steps of 1 fs each were run, followed by 5000 dynamics steps of 1 fs each, and then a VA09A energy minimization, typically with < 100 iterations. The conformation and the potential energy value were inspected after each minimization, and carbon–hydrogen atom distances were measured on the annealed, energy minimized final structure by means of the INSIGHT II/DISCOVER software. Prochiral configurations were determined by using the INSIGHT II/DISCOVER software.

Acknowledgements

Thanks are due Dr Joyce Graf for technical assistance.

References

[1] B. Coxon, *Carbohydr. Res.*, 13 (1970) 321–330.
[2] B. Coxon, *Carbohydr. Res.*, 322 (1999) 120–127.
[3] H.B. Sinclair, *J. Org. Chem.*, 44 (1979) 3361–3368.
[4] A.G. Palmer, III, J. Cavanagh, P.E. Wright, M. Rance, *J. Magn. Reson.*, 93 (1991) 151–170.
[5] J. Schleucher, M. Schwendinger, M. Sattler, P. Schmidt, O. Schedletzky, S.J. Glaser, O.W. Sorensen, C. Griesinger, *J. Biomol. NMR*, 4 (1994) 301–306.
[6] S.W. Homans, *Biochemistry*, 29 (1990) 9110–9118.
[7] B. Coxon, unpublished data.
[8] K. Tori, T. Komeno, T. Nakagawa, *J. Org. Chem.*, 29 (1964) 1136–1141.
[9] F.J. Weigert, J.D. Roberts, *J. Am. Chem. Soc.*, 89 (1967) 5962–5963.
[10] P. Dais, T.K. Shing, A.S. Perlin, *Carbohydr. Res.*, 122 (1983) 305–313.
[11] I. Bertini, C. Luchinat, in A.B.P. Lever (Ed.), *Coordination Chemistry Reviews: NMR of Paramagnetic Substances*, Vol. 150, Elsevier, Amsterdam, 1996, pp 266 and 291.
[12] P. Dais, *Adv. Carbohydr. Chem. Biochem.*, 51 (1995) 63–131.
[13] M. Karplus, *J. Chem. Phys.*, 30 (1959) 11–15.
[14] M. Karplus, *J. Am. Chem. Soc.*, 85 (1963) 2870–2871.
[15] C. Altona, C.A.G. Haasnoot, *Tetrahedron*, 13 (1980) 417–429.
[16] M. Barfield, *J. Chem. Phys.*, 41 (1964) 3825–3832.
[17] V.F. Bystrov, A.U. Stepanyants, *J. Mol. Spectrosc.*, 21 (1966) 241–248.
[18] B. Coxon, H.J. Jennings, K.A. McLauchlan, *Tetrahedron*, 23 (1967) 2395–2412.
[19] H. Booth, *Tetrahedron Lett.*, (1965) 411–416.
[20] R.L. Vold, J.S. Waugh, M.P. Klein, D.E. Phelps, *J. Chem. Phys.*, 48 (1968) 3831–3832.
[21] A.J. Shaka, J. Keeler, R. Freeman, *J. Magn. Reson.*, 53 (1983) 313–340.